

THE H I CONTENT OF LOCAL LATE-TYPE GALAXIES

C. EVOLI¹, P. SALUCCI¹, A. LAPI^{1,2}, AND L. DANESE¹

¹ SISSA, Via Bonomea 265, I-34136 Trieste, Italy; carmelo.evoli@sisssa.it

² Dipartimento di Fisica, Università di Roma “Tor Vergata,” Via della Ricerca Scientifica 1, I-00133 Rome, Italy
Received 2011 June 26; accepted 2011 October 17; published 2011 November 21

ABSTRACT

We present a solid relationship between the neutral hydrogen (H I) disk mass and the stellar disk mass of late-type galaxies in the local universe. This relationship is derived by comparing the stellar disk mass function from the Sloan Digital Sky Survey and the H I mass function from the H I Parkes All Sky Survey (HIPASS). We find that the H I mass in late-type galaxies tightly correlates with the stellar mass over three orders of magnitude in stellar disk mass. We cross-check our result with that obtained from a sample of HIPASS objects for which the stellar mass has been obtained by inner kinematics. In addition, we derive the H I versus halo mass relationship and the dependence of all the baryonic components in spirals on the host halo mass. These relationships bear the imprint of the processes ruling galaxy formation, and highlight the inefficiency of galaxies both in forming stars and in retaining their pristine H I gas.

Key words: galaxies: evolution – galaxies: formation – galaxies: statistics

Online-only material: color figures

1. INTRODUCTION

In recent years ground- and space-based surveys have allowed us to probe the physical properties of many millions of galaxies both in the local and the high-redshift universe. These analyses have been mainly focused on investigating the *stellar* component of galaxies, and have provided us with a much clearer view of when and where star formation occurred in cosmic time.

However, there is another baryonic component, namely the neutral atomic hydrogen H I, that should be accurately monitored to understand the process of galaxy formation; in fact, such a component constitutes the raw material which stars are made of. According to the standard picture, protogalactic halos initially all had the same cosmological amount of H I gas, around 1/6 of the host halo mass (e.g., Komatsu et al. 2011), in the form of a warm atmosphere. Then a fraction of such warm baryons is expected to cool and condense in a cold gaseous disk-like component, whereby stars are formed. In turn, this cold, star-forming gas can be depleted by energy feedback from Type II supernova (SN) explosions and stellar winds, in an amount modulated by the ratio between the total energy injected and the depth of the potential well of the host halo; notably, the former is related to the overall mass of stars formed and hence to the galaxy luminosity, while the latter crucially depends on the mass of the host halo (e.g., White & Rees 1978; Fall & Efstathiou 1980). At lower halo masses a large H I depletion is due to photoheating by the intergalactic UV radiation field (e.g., Hoefl et al. 2006; Ricotti 2009).

Therefore, observational information on the H I mass content of galaxies provides crucial constraints on galaxy formation theories; a successful scenario must be able to reproduce not only the observed stellar mass function and luminosity function (LF), but also the H I mass function (HIMF; Mo et al. 2005) and the relationships between the H I and the stellar/halo masses.

Only in recent years, thanks to the completion of relatively wide blind 21 cm surveys, have a large number of observations on H I gas become available. In detail, Zwaan et al. (2005) used the catalog of 4315 extragalactic H I 21 cm emission line detections from the H I Parkes All Sky Survey (HIPASS) to

obtain an accurate measurement of the galaxy HIMF down to an H I mass of $10^{7.2} M_{\odot}$.

In this work we aim to investigate the relationships between the H I mass and two relevant structural properties of late-type galaxies: the stellar disk and the halo masses. To do this we exploit (1) a theoretical approach that boils down to matching the cumulative HIMF mass function and the galactic stellar (or halo) mass function and (2) an observational approach that relies on a sample of objects for which both the H I and stellar disk masses have been measured *directly*. We show that the two approaches agree in indicating a strong correlation between the gaseous disk and stellar disk (or halo) mass.

The existence, in late-type spirals, of a relationship between the H I disk mass and the galaxy luminosity is well known (e.g., Roberts 1975; Roberts & Haynes 1994; Gavazzi et al. 1996; McGaugh & de Blok 1997; Disney et al. 2008), and so is that between the former and the spectrophotometrically derived mass of the stellar disk (Kannappan 2004; Gavazzi et al. 2008; Catinella et al. 2010). Recently, Cortese et al. (2011) showed that the H I-to-stellar mass ratio anticorrelates with stellar mass over ~ 2 orders of magnitude in stellar mass and investigated the effect of the environment on this relation.

Previous results, based on the spectrophotometric estimate of the stellar disk masses, have established the *existence* of the relations that are the object of the present investigation, but in a biased way. In fact, especially for spirals, the luminosity is a poor indicator of the stellar disk mass and, in any case, is uncertain by a factor of two (Salucci et al. 2008). In addition, it depends on the assumed initial mass function and star formation rate, quantities that we would like to study with the help of the results of this paper and not to assume a priori in order to get the results of this paper. Finally, the above relationships are biased by the fact that spirals with the same stellar disk mass, but overabundant or deficient in H I content, seem to have different stellar mass-to-light ratios (and then luminosities) than galaxies “normal” in H I content.

In this work, we aim to estimate the mass of a stellar disk, associated with an H I disk, in two essentially new, accurate, model-independent, and statistically relevant ways.

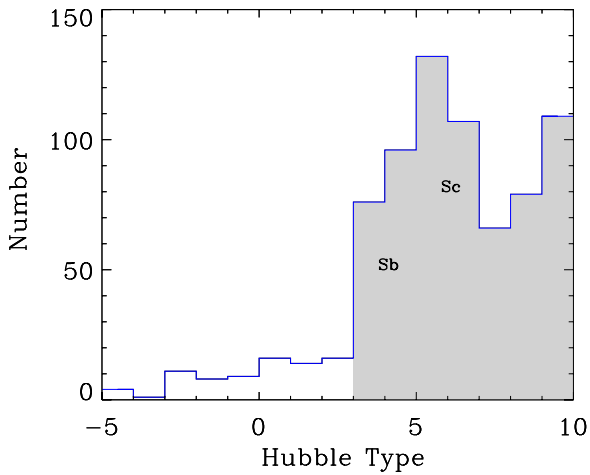


Figure 1. Distribution of Hubble types in the HIPASS galaxies as presented by Ryan-Weber et al. (2002).

(A color version of this figure is available in the online journal.)

These estimates are expected to yield reliable relationships or trends, free from biases that are likely to affect their interpretation in a cosmological context. Note that Shankar et al. (2006), by following Salucci & Persic (1999), were the first to correlate the kinematical bias-free estimates of stellar disk mass with the corresponding H I masses; however, their work was based on a much more limited sample, in terms of number of objects and magnitude extension, than the one we use in this work.

Finally, we apply the cumulative technique to derive the relationship between H I and halo masses. Even if not as strongly motivated as in the previous case, we are able to derive a more realistic relationship between these two observables with respect to what exists in the literature.

Throughout the paper we adopt the standard value $H_0 = 73 \text{ km s}^{-1} \text{ Mpc}^{-1}$ for the Hubble constant and quote uncertainties at the 1σ confidence level.

2. H I VERSUS STELLAR MASS RELATIONSHIP

To investigate the relationship between the stellar and the gas mass components in late-type galaxies, we follow the procedure of Vale & Ostriker (2004) and developed by Shankar et al. (2006). First, supported by the evidence described in Section 1, we assume that, on average, the mass of the H I disk is, in a statistical sense, an (increasing) monotonic function of the mass of the stellar disk.

If two galaxy properties q and p obey a one-to-one relationship, we can write

$$\phi(p) \frac{dp}{dq} dq = \psi(q) dq, \quad (1)$$

where $\psi(q)$ is the number density of galaxies with measured property between q and $q + dq$ and $\phi(p)$ is the corresponding number density for the variable p . The solution is based on a numerical scheme imposing that the number of galaxies with q above a certain value \bar{q} must be equal to the number of galaxies with p above \bar{p} , i.e.,

$$\int_{\bar{p}}^{\infty} \phi(p) dp = \int_{\bar{q}}^{\infty} \psi(q) dq. \quad (2)$$

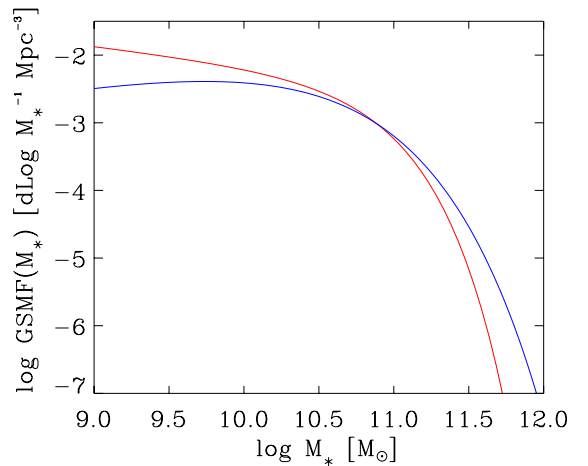


Figure 2. GSMF of late-type galaxies obtained from the LF by Bernardi et al. (2010) and the M/L ratios of Shankar et al. (2006) are illustrated as a blue line. The GSMF of Bell et al. (2003) is also shown (red line) for comparison.

(A color version of this figure is available in the online journal.)

In the following we take p as the H I mass M_{HI} and $\phi(p)$ as the corresponding HIMF, with q as the stellar mass M_* and $\psi(q)$ the corresponding galactic stellar mass function (GSMF).

The local HIMF has been measured by Zwaan et al. (2005) using the galaxy data in the HIPASS catalog (Meyer et al. 2004); its shape has been fitted, within the range $10^{7.2} M_{\odot} < M_{\text{HI}} < 10^{11} M_{\odot}$, with a Schechter function:

$$\phi(M_{\text{HI}}) dM_{\text{HI}} = \phi_{\text{HI}} \left(\frac{M_{\text{HI}}}{\tilde{M}_{\text{HI}}} \right)^{\alpha} \exp \left(-\frac{M_{\text{HI}}}{\tilde{M}_{\text{HI}}} \right) d \left(\frac{M_{\text{HI}}}{\tilde{M}_{\text{HI}}} \right) \quad (3)$$

with power-law slope $\alpha = -1.37 \pm 0.03$, characteristic mass $\log(\tilde{M}_{\text{HI}}/M_{\odot}) = 9.8 \pm 0.03 h_{75}^{-2}$, and normalization $\phi_{\text{HI}} = (6 \pm 0.8) \times 10^{-3} h_{75}^3 \text{ Mpc}^{-3} \text{ dex}^{-1}$.

Obviously, the two mass functions appearing in Equation (2) must be representative of the same galaxy population. To check this, we plot in Figure 1 the Hubble-type distribution (obtained from the HyperLeda Catalogue; see Paturel et al. 2003) of the 1000 brightest HIPASS galaxies as reported in Ryan-Weber et al. (2002). We conclude that the HIMF represents almost entirely disk systems: late-type galaxies account for more than 85% (Sb–Sc), there is a small contribution from irregular galaxies (smaller than 15%), and the contribution from ellipticals is negligible (smaller than 2%).

Thus, we calculate the GSMF for late-type and irregular galaxies on the basis of the recent observational results reported in Bernardi et al. (2010). Specifically, we use their LF for $C_r < 2.6^3$ (M. Bernardi 2011, private communication), which implies a small contamination from early-type galaxies, around 2% from ellipticals, and less than 26% from Sa-type objects. From this we build the GSMF by adopting the *disk* mass-to-light ratio derived from mass modeling of the (spiral) universal rotation curve, see Equation (2) in Shankar et al. (2006), and we fit it with a modified Schechter function (see Bernardi et al. 2010, Equation (9)):

$$\phi(M_*) dM_* = \phi_* \left(\frac{M_*}{\tilde{M}_*} \right) \frac{e^{-(M_*/\tilde{M}_*)^{\beta}}}{\Gamma(\alpha/\beta)} \beta d \left(\frac{M_*}{\tilde{M}_*} \right) \quad (4)$$

with parameters $\phi_* = 1.05 \times 10^{-2} \text{ Mpc}^{-3}$, $\alpha = 0.385$, $\beta = 0.59$, and $\log \tilde{M}_* = 10.05$. The function is plotted in Figure 2

³ C_r is the concentration index defined as the ratio of the scale which contains 90% of the Petrosian light in the r band to that which contains 50%.

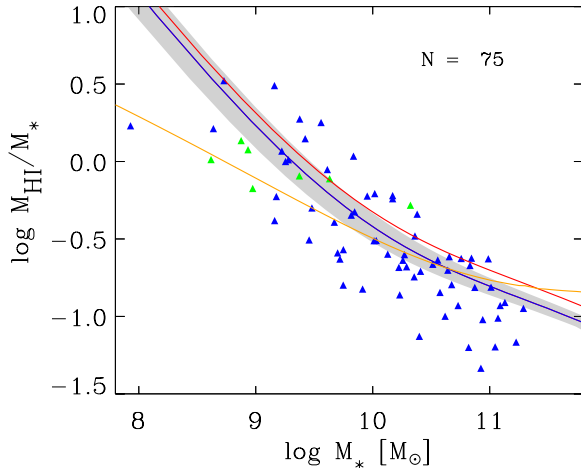


Figure 3. Ratio of H I-to-stellar disk mass as a function of stellar disk mass; the dashed area represents the uncertainty related to HIMF normalization. Triangles represent individual objects (blue symbols are for late types and green for irregulars). Red and orange lines show the effects of changing the HIMF and the GSMF, respectively, as described in Section 2. The H₂-to-stellar mass ratio is also reported as a green line.

(A color version of this figure is available in the online journal.)

alongside, for the sake of comparison, the GSMF of late-type galaxies obtained by Bell et al. (2003) from model-dependent spectrophotometric estimates of the disk masses. The method we use suffers from a number of different uncertainties, in particular in inferring stellar masses from kinematical measurements; hence the total uncertainty in our results is of the order of 30%.

More recently, the ALFALFA collaboration has published an HIMF based on 10,119 galaxies by probing a volume bigger than HIPASS (Martin et al. 2010). The new HIMF differs from the HIPASS one at the high-mass end, which changes the normalization of the H I-to-stellar mass ratio. We show in Figure 3 that the differences in assuming the ALFALFA HIMF are within the error bars associated with the uncertainties in the HIPASS HIMF normalization.

Then, we solve Equation (2) and derive the relationship between the gas-to-star fraction and the stellar mass; the result is shown in Figure 3. The gas fraction and the stellar mass correlate as a broken power law over about three orders of magnitude in stellar mass. Within the mass range $10^8 < M_* < 10^{11}$, the relationship can be well approximated by

$$\frac{M_{\text{HI}}}{3.36 \times 10^9 M_{\odot}} = \left(\frac{M_*}{3.3 \times 10^{10} M_{\odot}} \right)^{0.19} \times \left[1 + \left(\frac{M_*}{3.3 \times 10^{10} M_{\odot}} \right)^{0.76} \right]. \quad (5)$$

This relationship, obtained by direct estimation of the stellar disk mass, can be compared with that obtained by means of the (biased) traditional methods. In Figure 3, we compare our result with the H I-to-stellar mass obtained by using the Bell et al. (2003) GSMF. The difference between the two is particularly pronounced at small masses, where the spectrophotometric M/L ratios of Bell et al. (2003) are appreciably larger than the kinematical estimates.

3. H I CONTENT OF INDIVIDUAL GALAXIES

We derive the relationship between the H I mass (M_{HI}) and the stellar disk mass (M_{D}) with a new model-independent method by looking at *individual* late-type galaxies. The disk mass is obtained, within a reasonable uncertainty, by modeling the galaxy rotation curve, whose inner parts are decomposed into halo and disk components.

Let us first define $R_{\text{opt}} \equiv 3.2R_{\text{D}}$, where R_{D} is the exponential thin disk length scale. This radius, that encloses about 83% of the total light, can be considered as the physical size of the stellar disk. Persic & Salucci (1990) devised a reliable method to estimate the disk mass from observational quantities, i.e., from the gravitating mass M_{g} inside R_{opt} ($M_{\text{g}} \approx G^{-1} V_{\text{opt}}^2 R_{\text{opt}}$) and the rotation curve logarithmic slope at R_{opt} (∇):

$$M_{\text{D}} = (0.72 - 0.85 \nabla) M_{\text{g}}. \quad (6)$$

We then proceed to build a sample containing 75 objects in HIPASS that have optical photometry and kinematics of quality sufficient for the above method. The rotation curves are taken from Persic & Salucci (1995), Yegorova & Salucci (2007), and Frigerio Martins & Salucci (2007). By means of Equation (6) we derive the disk mass with an uncertainty between 10% and 30% (Persic & Salucci 1990).

In Figure 3, we show the relation obtained for individual objects and that obtained by matching the HIMF to the GSMF. The two are in very good agreement over two orders of magnitude in stellar mass, showing the same power-law functional form (with a slope, respectively, of -0.48 and -0.52) and similar normalization. The agreement between individual objects and the statistical relation, obtained from two very different methods, indicates that the first one is little biased by contamination or incompleteness of the HIMF, and that the second uses a fair sample of individual objects. A stellar disk mass versus H I disk mass relation emerges as one of the most important empirical relationships concerning spirals.

A further gas component in the local galaxies is the molecular hydrogen (H₂) disk. Although we must caveat that its mass does not necessarily correlate monotonically with the stellar disk mass (e.g., Casoli et al. 1996; Boselli et al. 2002; Böker et al. 2003), we will proceed as above, since more information on this poorly known component is certainly needed.

Let us stress that, unlike the H I mass, the H₂ disk mass estimate relies on indirect tracers such as CO lines, with uncertain conversion factors. We adopt the H₂MF derived by Obreschkow & Rawlings (2009) from the local CO LF of the CARO Extragalactic CO Survey, assuming a variable CO-to-H₂ conversion factor fitted to nearby observations. The corresponding mass function (H₂MF) is well fitted by a Schechter function with power-law slope $\alpha = -1.07$, characteristic mass $\log(M_{\text{H}_2}/M_{\odot}) = 9.2$, and normalization $\phi_{\text{H}_2} = 8.3 \times 10^{-3} \text{ Mpc}^{-3} \text{ dex}^{-1}$. The resulting H₂-to-stellar mass ratio as a function of the stellar mass is shown in Figure 3: as expected, this component turns out to be subdominant relative to H I over the whole mass range probed and for this reason we do not consider this contribution in the rest of the paper.

4. H I VERSUS HALO MASS RELATIONSHIP

It is cosmologically relevant to derive the relationship between H I mass M_{HI} and halo mass M_{H} in spirals. A preliminary step is to obtain the relationship between the stellar mass M_* and halo mass M_{H} by the method described in Section 2. Shankar

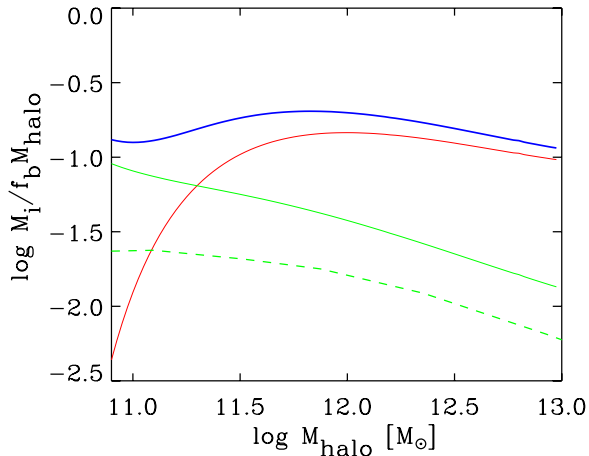


Figure 4. Baryonic content relative to the initial baryonic mass associated with a halo ($f_b M_{\text{halo}}$). The red line refers to stars, the green line to H I, and the blue line to the total. The dashed line shows the finding of Marín et al. (2010).

(A color version of this figure is available in the online journal.)

et al. (2006) have already obtained these results but it is worth re-performing their analysis with updated observational data. For this purpose, we need two ingredients. The first is the galactic halo mass function (HF), i.e., the statistics of halos containing one single galaxy; Shankar et al. (2006) evaluated this from the standard halo mass function by adding the contribution of subhalos and subtracting the contribution of galaxy systems (see their Equation (9)). The second is the GSMF of all the local galaxy population, necessary because the HF does not distinguish between galaxy morphology. We use the GSMF of Bernardi et al. (2010) without selection criteria for the concentration index; this is fitted in terms of a modified Schechter function (see their Equation (9)) with parameters given in their Table B5.

The relationship derived with these mass functions holds for the overall galaxy population, so to proceed further we must assume that it also holds approximately for each separate Hubble type, in particular, for *late-type* objects. This is justified by the fact that we found that the fractional amount of the H I component with respect to the whole baryonic component varies across spirals by three orders of magnitude; on the other hand, from X-ray and weak-lensing observations, we can infer that galaxies with the same halo mass have approximately the same baryonic mass and that, furthermore, the relation between the galaxy virial mass and the relative baryonic mass is roughly independent of Hubble type (Fukazawa et al. 2006; Nagino & Matsushita 2009; Donato et al. 2009).

Thus, we combine the H I versus stellar mass relationship with the stellar versus halo mass relationship to obtain the H I versus halo mass relationship. We show the result in Figure 4; the relation can be fitted (to better than 5% in comparison with the numerical result) within the mass range $10^{11} M_{\odot} < M_{\text{H}} < 10^{12.5} M_{\odot}$ as

$$\frac{M_{\text{H I}}}{9 \times 10^9 M_{\odot}} = \frac{(M_{\text{H}}/9.5 \times 10^{11} M_{\odot})^{0.33}}{1 + (M_{\text{H}}/9.5 \times 10^{11} M_{\odot})^{-0.77}}. \quad (7)$$

We also plot for comparison the H I versus halo mass relationship recently derived by Marín et al. (2010) by comparing directly the statistics of H I and halo masses. Their results differ appreciably from ours since the standard halo mass function they adopt includes the contribution of galaxy group systems so it has more objects relative to our GHMF; then, the matching procedure in Section 2 leads to a lower H I mass at a given halo mass.

In Figure 4, we summarize our results by showing the amount of H I and stellar mass (relative to the initial baryonic mass) associated with a halo as a function of its virial mass. We also plot the overall baryon fraction derived by adding the stellar mass to the total gas mass obtained by multiplying the H I mass by 1.4 to take into account the contribution of He.

5. DISCUSSION AND CONCLUSIONS

The correlations of the H I mass with stellar and halo masses are extremely relevant in the framework of galaxy formation theories. The standard picture envisages that every galaxy forms with the same initial amount of baryons in the form of H I gas, and what we observe now are the remains of processes that took place during galaxy formation.

Figure 4 shows that late-type galaxies are extremely inefficient in retaining their initial baryon content, i.e., most of the initial H I gas has been removed from the host halo. Less than 10% is retained in galaxies with halo masses below $10^{11} M_{\odot}$, and this value drops to few percent for halo masses above $10^{12} M_{\odot}$. Such a behavior is likely due to SN feedback. Thus only a small fraction of the initial baryon content is eventually exploited for star formation. Note that, in massive halos, stars are the dominant baryonic component while in smaller halos H I gas is.

Let us stress, however, that the baryon cycle in spirals is very complicated to understand. It may depend, in addition to SN feedback, IGM (intergalactic medium) ionization, and gas cooling time, on the interplay between galaxies and their environment, especially for low-mass halos. Note smoothed particle hydrodynamics simulations have not yet converged to a definitive result: e.g., Hoeft et al. (2006) find that halos with $M > 10^{10.5} M_{\odot}$ are able to retain all their baryons while Pilkington et al. (2011) find that the galaxy formation process is able to remove most of the original baryonic material. All this means that the processes that are responsible for the evolution of galactic gas about which this paper provides valuable information are not fully understood.

One can wonder why this gas, although not being ejected by SN feedback, has not been used for star formation. To answer the question, we look at where this residual H I gas is presently residing by highlighting in the previous correlations the contribution from the H I gas located inside or outside the stellar disk radius R_{opt} . Therefore, we model the gas surface density of late-type galaxies with the functional form observed in most spirals (see, e.g., Bigiel et al. 2010):

$$\log \Sigma = \begin{cases} \log \Sigma_0 & \text{if } r \leq R_{\text{opt}} \\ \log \Sigma_0 - 2(r - R_{\text{opt}})/(R_f - R_{\text{opt}}) & \text{if } r > R_{\text{opt}}, \end{cases} \quad (8)$$

where R_f is the radius at which the surface density drops to 1/100 of the value at R_{opt} that we assume as the size of the H I disk and Σ_0 is the H I surface density central value.

We need now to relate the length scale of the stellar distribution to that of the neutral gas. Note that our aim is to obtain qualitative results; in this view the assumptions we take are well justified. Broeils & Rhee (1997) and Rhee & van Albada (1996) published the H I surface density profiles for 60 spirals of known optical radii R_{opt} and blue luminosity L_B (that are given in Table 1 of Rhee & van Albada 1996; note that the quantity in the fourth column is $\simeq R_{\text{opt}}/2$). From these measurements they derived (1) the H I half-mass radius R_{eff} and (2) the total mass $M_{\text{H I}}$ (given in Columns 5 and 6 of the same table). From these quantities we obtain a strong R_{eff} versus R_{opt} relationship and, by the definition of R_{eff} , the relationship $R_f = F(R_{\text{eff}}(R_{\text{opt}}), R_{\text{opt}})$. Moreover, to

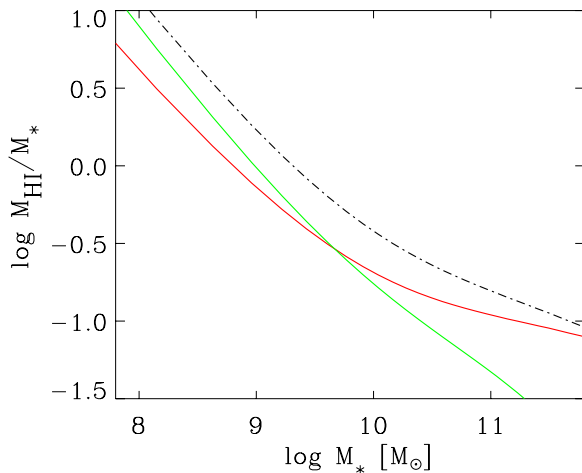


Figure 5. Red line shows the H I mass inside the optical radius, the green line the H I mass outside, and the black line the total.

(A color version of this figure is available in the online journal.)

transform light in stellar mass, we use, without loss of generality, $M_* = 10^{11} (L_B / 10^{11} L_\odot)^{1.4} M_\odot$ (Salucci et al. 2007). Finally, by combining and manipulating the above empirical relationships (which also implies assuming Equation (8)), we obtain

$$R_f / R_{\text{opt}} = 3 - 2/3 \log (M_* / 10^9 M_\odot) . \quad (9)$$

The above relation indicates, not surprisingly, that small galaxies have a larger H I disk in terms of the stellar disk size. In Figure 5, we show how the H I mass is divided into that inside and outside R_{opt} , the radius inside which the stars reside. The former is the dominant component for massive objects, while the latter gives a dominant contribution in small galaxies.

The overabundance of H I over stellar mass in small objects is due to material located far away the stellar disk and mostly unprocessed. It is worth noticing that in these objects at these radii the H I surface density is much lower than the threshold of order $1 M_\odot \text{ kpc}^{-2}$ needed by the Toomre criterion to form stars. This H I component has not been at the disposal of the latter process and it never will. Let us stress that the inefficiency of the star formation process in the outer regions of disks is directly probed (Bigiel et al. 2010).

To sum up, in this work we have derived robust correlations between the H I and stellar (halo) mass for late-type galaxies in the local universe. These relationships bear the imprint of the processes ruling galaxy formation (see Cook et al. 2010 for a theoretical approach that considers them) and highlight the inefficiency of galaxies both in forming stars and in retaining their pristine H I gas.

We acknowledge M. Bernardi for having provided us with the LF data for late-type galaxies. This work is partially supported by MIUR, INAF, and ASI. A.L. thanks SISSA and INAF-OATS for warm hospitality.

REFERENCES

- Bell, E. F., McIntosh, D. H., Katz, N., & Weinberg, M. D. 2003, *ApJS*, **149**, 289
- Bernardi, M., Shankar, F., Hyde, J. B., et al. 2010, *MNRAS*, **404**, 2087
- Bigiel, F., Leroy, A., Walter, F., et al. 2010, *AJ*, **140**, 1194
- Böker, T., Lisenfeld, U., & Schinnerer, E. 2003, *A&A*, **406**, 87
- Boselli, A., Lequeux, J., & Gavazzi, G. 2002, *Ap&SS*, **281**, 127
- Broeils, A. H., & Rhee, M. 1997, *A&A*, **324**, 877
- Casoli, F., Dickey, J., Kazes, I., et al. 1996, *A&A*, **309**, 43
- Catinella, B., Schiminovich, D., Kauffmann, G., et al. 2010, *MNRAS*, **403**, 683
- Cook, M., Evoli, C., Barausse, E., Granato, G. L., & Lapi, A. 2010, *MNRAS*, **402**, 941
- Cortese, L., Catinella, B., Boissier, S., Boselli, A., & Heinis, S. 2011, *MNRAS*, **415**, 1797
- Disney, M. J., Romano, J. D., Garcia-Appadoo, D. A., et al. 2008, *Nature*, **455**, 1082
- Donato, F., Gentile, G., Salucci, P., et al. 2009, *MNRAS*, **397**, 1169
- Fall, S. M., & Efstathiou, G. 1980, *MNRAS*, **193**, 189
- Frigerio Martins, C., & Salucci, P. 2007, *MNRAS*, **381**, 1103
- Fukazawa, Y., Botoya-Nonesca, J. G., Pu, J., Ohto, A., & Kawano, N. 2006, *ApJ*, **636**, 698
- Gavazzi, G., Giovanelli, R., Haynes, M. P., et al. 2008, *A&A*, **482**, 43
- Marín, F. A., Gnedin, N. Y., Seo, H., & Vallinotto, A. 2010, *ApJ*, **718**, 972
- Martin, A. M., Papastergis, E., Giovanelli, R., et al. 2010, *ApJ*, **723**, 1359
- McGaugh, S. S., & de Blok, W. J. G. 1997, *ApJ*, **481**, 689
- Meyer, M. J., Zwaan, M. A., Webster, R. L., et al. 2004, *MNRAS*, **350**, 1195
- Mo, H. J., Yang, X., van den Bosch, F. C., & Katz, N. 2005, *MNRAS*, **363**, 1155
- Nagino, R., & Matsushita, K. 2009, *A&A*, **501**, 157
- Obreschkow, D., & Rawlings, S. 2009, *MNRAS*, **394**, 1857
- Paturel, G., Petit, C., Prugniel, P., et al. 2003, *A&A*, **412**, 45
- Persic, M., & Salucci, P. 1990, *ApJ*, **355**, 44
- Persic, M., & Salucci, P. 1995, *ApJS*, **99**, 501
- Pilkington, K., Gibson, B. K., Calura, F., et al. 2011, *MNRAS*, in press
- Rhee, M.-H., & van Albada, T. S. 1996, *A&AS*, **115**, 407
- Ricotti, M. 2009, *MNRAS*, **392**, L45
- Roberts, M. S. 1975, in *Radio Observations of Neutral Hydrogen in Galaxies*, ed. A. Sandage, M. Sandage, & J. Kristian (Chicago, IL: Univ. Chicago Press), 309
- Roberts, M. S., & Haynes, M. P. 1994, *ARA&A*, **32**, 115
- Ryan-Weber, E., Koribalski, B. S., Staveley-Smith, L., et al. 2002, *AJ*, **124**, 1954
- Salucci, P., Lapi, A., Tonini, C., et al. 2007, *MNRAS*, **378**, 41
- Salucci, P., & Persic, M. 1999, *MNRAS*, **309**, 923
- Salucci, P., Yegorova, I. A., & Drory, N. 2008, *MNRAS*, **388**, 159
- Shankar, F., Lapi, A., Salucci, P., De Zotti, G., & Danese, L. 2006, *ApJ*, **643**, 14
- Vale, A., & Ostriker, J. P. 2004, *MNRAS*, **353**, 189
- White, S. D. M., & Rees, M. J. 1978, *MNRAS*, **183**, 341
- Yegorova, I. A., & Salucci, P. 2007, *MNRAS*, **377**, 507
- Zwaan, M. A., Meyer, M. J., Staveley-Smith, L., & Webster, R. L. 2005, *MNRAS*, **359**, L30